International Symposium of Research Students on Materials Science and Engineering
December 20-22, 2004, Chennai, India
Department of Metallurgical and Materials Engineering, Indian Institute of Technology Madras

LOW CYCLE FATIGUE BEHAVIOR OF A MODIFIED 9Cr-1 Mo FERRITIC STEEL

Vani Shankar, M.Valsan, R.Kannan, K.Bhanu Sankara Rao, S.L.Mannan and S.D.Pathak*
Metallurgy and Materials Group,
Indira Gandhi Centre for Atomic Research, Kalpakkam-603102, Tamil Nadu
** Indian Institute of Technology Madras, Chennai-600 036, Tamil Nadu*

ABSTRACT

Fatigue at elevated temperatures is influenced by various time and temperature dependent damage processes such as creep, oxidation, phase transformations and dynamic strain ageing (DSA) in the temperature range of their operation. In this paper the detrimental effects of DSA and oxidation in high temperature LCF is discussed with reference to extensive studies on Mod. 9Cr-1Mo steel. DSA is reported to enhance the stress response and reduce ductility. It localizes fatigue deformation, enhances fatigue cracking and reduces fatigue life. High temperature oxidation is found to accelerate transgranular and intergranular fatigue cracking in Mod. 9Cr-1Mo steel. In this paper, influence of temperature, strain amplitude and strain rate on the LCF behaviour of a modified 9Cr-1Mo ferritic steel in the normalized and tempered condition is reported. Total axial strain controlled LCF tests at various strain amplitudes such as ±0.25%, ±0.4%, ±0.6% and ±1% at constant strain rate of 3×10^{-3} s^{-1} were carried out in the temperature range 773 K-873 K. Influence of strain rate was studied employing strain rates of 3×10^{-4}, 3×10^{-3} and 3×10^{-2} s^{-1} in the temperature range, 773 to 873 K at a fixed strain amplitude of ±0.6%. Fatigue life was found to decrease with increase in the testing temperature and decrease in strain rate where oxidation-assisted crack initiation and propagation contributed to life reduction.

Keywords: low cycle fatigue, strain rate, temperature, dynamic strain aging

1. INTRODUCTION

Plain 9Cr-1Mo ferritic steel modified with alloying additions of niobium and vanadium and controlled amount of nitrogen is extensively used as a high temperature structural material for a variety of applications including steam generators of liquid metal cooled fast breeder reactors[1]. High thermal conductivity and low thermal expansion coefficient coupled with enhanced resistance to stress corrosion cracking in steam-water systems have favoured the selection of this steel for these applications. The material also possesses better monotonic tensile and creep strengths at elevated temperatures compared with the plain 9Cr-1Mo steel. The alloy also exhibits good weldability and microstructural stability over very long periods of exposure to high temperature service conditions.

The addition of Nb improves the properties by promoting nucleation of finely distributed $M_{23}C_6$ carbides and by aiding grain size refinement, whereas V enters the carbide particles and retards their growth. It must be mentioned that in this alloy, strength in normalized and tempered condition is derived from carbides like NbC, VC and $M_{23}C_6$ on sub-boundaries and from the tempered martensitic laths with high dislocation densities. In addition, V and Cr could also form fine precipitates of nitrides within the ferrite matrix contributing to further strengthening[2-5]. Mo is a solid solution strengthener and is considered a retardant for dislocation recovery/recrystallisation[6].

The components of the steam generators, which are designed for a life span of 30 to 40 years, are often subjected to repeated thermal stresses as a result of temperature gradients that occur on heating

and cooling during start-ups and shut-downs or during temperature transients while the reactor is in operation. Steady state operation in between start-up and shut-down or transients would produce creep effects and therefore the low cycle fatigue (LCF) and creep-fatigue interaction are important considerations in the design of these components. The LCF behaviour of this steel has been reported earlier under Normalized and Tempered[4,7-13] and thermally aged conditions[6,14,15]. Further, detailed investigations have been carried out to evaluate the creep-fatigue interaction behaviour of the alloy[6,7,14-17]. Ebi and Mc Evily[4] showed that the hot forged alloy exhibits inferior fatigue properties at 811K as compared to the fine-grained, hot-rolled material. It was concluded that the coarse grain size adversely affects the fatigue crack initiation stage but has little effect on the crack propagation. Prolonged ageing of the alloy at elevated temperatures prior to testing was found to reduce the LCF and creep-fatigue interaction lives[6,15]. Ageing resulted in the formation of Laves phase with associated reduction in the toughness and LCF lives of the alloy[6,15]. Studies on the influence of strain hold position on the creep-fatigue life indicated that the hold in compression peak strain was more deleterious than that in tension. This was attributed to the detrimental effect of oxide behaviour in compression hold[17]. Life was observed to decrease with increase in the dwell time up to 1 hour under tension hold beyond which there was an apparent saturation[6]. During long time creep tests, carbide coarsening and coalescence at grain boundaries was found to introduce intergranular damage in the alloy[18].

In the present paper the current understanding developed on the effects of temperature, strain range and strain rate on the LCF behaviour of modified 9Cr-1Mo steel is presented.

2. EXPERIMENTAL

Modified 9Cr-1Mo steel (Grade 91) used in this investigation had the following chemical composition(%): Cr 8.2 , Mo 0.92, C 0.11, V 0.13, Nb 0.09, Mn 0.48, Si 0.3, S 0.005, P 0.018, N 0.051, Ni 0.12, Al 0.015, Co 0.015, Cu 0.05 and Fe balance. The steel was obtained in the form of extruded tube of 30mm wall thickness. Blanks of 110 mm were cut and were given normalizing treatment at 1313 K/1hour + air cooling followed by tempering at 1033 K for 1 hour + air cooling. Specimens of 25 mm gauge length and 10 mm gage diameter were machined from the heat-treated rods and were tested at a constant strain rate of 3×10^{-3} s^{-1} at different strain amplitudes (±0.25% to ±1.0%) in the temperature range 773 K-873 K. Influence of strain rate was studied employing strain rates of 3×10^{-4}, 3×10^{-3} and 3×10^{-2} s^{-1} in the temperature range, 773 to 873 K at a fixed strain amplitude of ±0.6%. Tests were carried out in air under total axial strain control mode using an Instron 1343 servo hydraulic machine, equipped with a radiant heating furnace. The fatigue crack initiation and propagation behaviours under different testing conditions were studied using optical and scanning electron microscopy. Samples for the optical metallography were etched using Vilella's reagent (1g of picric acid + 5ml conc. HCl + 100ml ethyl alcohol) and examined under an optical microscope. Samples for transmission electron microscopy was prepared by mechanically thinning samples to 100 μm thickness and finally electrolytic thinning using a double jet electropolisher. Transmission electron microscopic studies were carried out using Philips CM200 microcope operating at 200 KV.

3. RESULTS AND DISCUSSION

The alloy in the normalized and tempered state exhibited a tempered martensitic structure, Fig.1. The martensite lath boundaries were found decorated with isolated and very fine $M_{23}C_6$ particles.

3.1 CYCLIC PROPERTIES

The cyclic stress response of the alloy at different strain amplitudes at 823 K and strain rate 3×10^{-3} s^{-1} is presented in Fig. 2. This material generally shows a cyclic softening behavior, so in the first few cycles in the beginning, the stress dropped quickly, then approached a stable state (i.e. saturated stress) The stress saturation period was found to increase with decrease in strain amplitude. The stress plateau continued till the onset of final load drop, which occurs due to the initiation and propagation of fatigue cracks. Further, the stress response was found to decrease with increase in test temperature as shown in Fig. 3. At 873 K, the alloy showed secondary hardening in its stress response. Fig. 4 shows the effect of strain rate on the cyclic stress response at different temperatures such as 773 K, 823 K and 873 K. The material showed continuous softening regime at almost all the temperatures and strain rate. At 873 K, the alloy showed secondary hardening in its stress response. However an initial brief hardening followed by a continuous softening regime occurs at some temperature and strain rate combination namely 773 K at $3x10^{-2}$ s^{-1} and $3x10^{-3}$ s^{-1} and at 823 K at $3x10^{-2}$ s^{-1}. The initial hardening could result from either individual or combined effects of: (1) mutual interaction among dislocations, (2) formation of fine precipitates on dislocations during testing and (3) dynamic strain ageing (DSA) as a consequence of interaction between dislocations and solute atoms. It is possible that at higher temperatures, the formation of fine precipitates on dislocations and matrix during testing could contribute to the initial cyclic hardening. However, the initial hardening occurs only during the faster strain rates where the testing time is not sufficient to cause precipitation.

Alloys which exhibit DSA often show one or more of the following deformation features, in addition to serrated flow; plateaus in the monotonic flow stress-temperature curves, high monotonic work hardening rates which increase with temperature, negative strain rate sensitivity of flow stress and ductility minima.

At intermediate temperatures, where the effects of time dependent processes such as creep and oxidation are found to be minimal, the drastic reduction in LCF life observed with increasing temperature and decreasing strain rate in alloys such as Nimonic PE 16 superalloy[19], Haynese 188 superalloy[20], Hastealloy[21] and Duplex stainless steel[22] has been ascribed primarily to the deleterious effects of DSA.

The effect of DSA on mechanical behaviour of austenitic stainless steels has been studied by several investigators. LCF tests on 304 SS[23] had shown that dynamic strain ageing manifested in LCF in the form of increase in tensile peak stress with increasing temperature, increase in half-life stress with decreasing strain rate, increased cyclic hardening rate and serrations in the plastic portions of stress-strain hysteresis loops [23-25]. Fatigue life was found to decrease significantly with decrease in strain rate at 823 K, due to DSA effects. Dynamic strain ageing caused intergranular cracking and the associated reduction in fatigue life. At 923 K, reduction in fatigue life was attributed to deleterious effects of oxidation and DSA. The effect of DSA on cyclic behaviour of 304 SS has also been studied by TSuzaki et al [24], at various strain rates and temperatures. They have observed serrations at lower temperatures during cyclic deformation than in monotonic tensile deformation.

The present alloy did not exhibit serrations in the plastic portions of stress-strain hysteresis loops in the temperature range examined.Studies by Nagesha et al [25], have observed serrations during LCF deformation at lower strain rate (3×10^{-4} s^{-1}) at 773 K. In tensile deformation at a strain rate of 3×10^{-4} s^{-1}, serrations were observed between 523 and 673 K, and at a strain rate of 3×10^{-3} s^{-1}, they were noticed at 623 K. In the present investigation, in the fatigue deformation taking place at a higher strain

rate of 3×10^{-3} s^{-1}, the operative temperature range for DSA could get shifted to higher temperature values.

The cyclic softening of this material observed in major portion of the life in general, agrees with the reported observations in high strength materials. Cyclic softening has been found earlier in the case of plain and modified 9Cr-1Mo steels[4,6,9,26,27]. Jones and Van Den Avyle[28] have reported from their investigations on 2.25Cr-1Mo steels that cyclic loading-induced dislocation shuttling accelerates the formation of Mo-C-Mo clusters eventually leading to the replacement of Mo-C pairs; the consequent loss of interaction solid solution hardening as the cause of cyclic softening. The mechanisms that have been suggested to explain the softening in these steels based on extensive substructural investigations include: (i) annihilation of dislocations introduced during martensitic transformation, (ii) change from the original lath structure to cells or equi-axed subgrains, (iii) degradation of strength due to coarsening of precipitates, (iv) replacement of Mo-C pairs by Mo-C-Mo clusters with an associated loss in interaction solid solution hardening and (v) stress reduction associated with the surface oxide film formation during deformation[14, 24].

3.2 CYCLIC STRESS-STRAIN BEHAVIOR AND FATIGUE LIFE

Figure 5 represents the variation of plastic strain range versus number of cycles to failure for continuous cycling at three test temperatures. This follows Coffin-Manson relationship represented by equation below

$$\frac{\Delta\varepsilon_p}{2} = \varepsilon_{f'}(2N_f)^c$$

where $\Delta\varepsilon_p/2$ is the plastic strain amplitude, $2N_f$ is the number of reversals to failure, $\varepsilon_{f'}$ is the fatigue ductility coefficient and c is the fatigue ductility exponent. The alloy exhibited a decrease in fatigue life with increasing temperature. Table I gives the half–life plastic strain amplitude and half-life tensile stress values at the three test temperatures. Whereas peak stress decreased with increase in temperature, no such conclusion could be drawn from the plastic strain values obtained from the hysteresis loops of the half-life cycle.

In order to identify the influence of DSA on the cyclic behavior of Mod. 9 Cr-1 Mo steel, the half life tensile stress and maximum tensile stress obtained during cycling were examined as function of strain rates. Fig. 6 shows peak at intermediate strain rate at all the three test temperatures. The lower peak stress for slower strain rates are described as “normal” behavior[29]. However, in the intermediate temperature region, an anomalous behavior observed as the higher peak tensile stress corresponding to the slower stress strain rates is ascribed to be due to the strengthening effects of DSA. In the temperature range from 773 K to 823 K, solute atoms acquire enough mobility to diffuse to the dislocation cores producing a drag effect on the mobile dislocation . This drag effect will be more pronounced for the slowest dislocation velocity. Thus at 773 K and 823 K, the peak stress increases when the strain rate is decreased from 3×10^{-2} s^{-1} to 3×10^{-3} s^{-1}. However, during 3×10^{-4} s^{-1} strain rate test, the synergistic process between high temperature and mechanical cycling improves the recovery process promoting the development of the an equiaxed subgrain structure leading to a lower dislocation density[29].

Further, fatigue life decreased with decreasing strain rate and showed a least value at slowest strain rate of 3×10^{-4} s^{-1} at both 773 K and 823 K (Fig. 7). The optical micrograph in Fig. 8 (c) shows cracks filled with oxide debris obtained in low strain rate testing conditions. It may be mentioned that the lower strain rates at elevated temperature provide adequate time for the environmental interaction to take place, which accelerates both the crack initiation and propagation phases. In contrast, under conditions of low temperatures oxidation effects were not significant (Fig. 8 (a)). The detrimental effect of oxidation was reflected vividly in Fig. 9. In modified 9Cr-1Mo steel, the oxide layer formed on the surface of the specimen is a weak barrier that can be easily overcome by slip. Ebi and McEvily[4]

studied the influence of air environment on stage II crack growth in modified 9Cr-1Mo steel by comparing the air and vacuum test results. It was found that the surface of the specimen tested in vacuum was much more rumpled compared to that when tested in air. Also, several crack initiation sites were observed in the air-tested specimen whereas in vacuum-tested specimens secondary cracks were found to be less. Challenger and Miller proposed a fall in threshold for crack propagation associated with the brittle oxides formed in a 2.25Cr-1Mo steel[30]. Ogata and Nitta[31] have used a similar concept, coupled with the wedge effect of exfoliated oxide, to explain the oxidation-assisted cracking in modified 9Cr-1Mo steel under creep-fatigue interaction conditions. The reduction in the LCF life under high temperature and low strain rate conditions could thus be ascribed to the enhanced environmental effects. Both crack initiation and propagation were seen to be transgranular under all the testing conditions investigated. This is to be expected since the 9Cr ferritic steels are generally known to resist grain boundary cavitation and associated intergranular failure even under creep-fatigue conditions[3].

CONCLUSIONS

1. Cyclic stress response of modified 9Cr-1Mo steel in normalized and tempered condition was characterized by initial hardening followed by softening. Hardening is attributed to dynamic strain ageing effects and precipitation at high temperatures. Cyclic softening is ascribed to the coarsening of precipitates and other microstructural changes.
2. DSA effects are prominent under specific temperature, strain rate and strain amplitude combination.
3. Manifestations of DSA such as increase in peak tensile stress and half-life stress at intermediate strain rates were observed in the present study.
4. Oxidation was found to have detrimental influence on fatigue life at low strain rates testing and high temperature.

REFERENCES

1. C.R. Brinkman, B. Gieseke and P.J. Maziasz, *Microstructure and Mechanical properties of Ageing Material* eds. P.K. Liaw, R. Viswanathan, K.L. Murty, E.P. Simonen and D. Frear, The Minerals, Metals and Materials Society (1993) 107.
2. V.K. Sikka, *Proceedings of Topical Conference on Ferritic Alloys for use in Nuclear Energy Technologies*, eds. J.W. Davis and D.J. Michel, Snowbird, Utah, June 19-23(1983) 17.
3. S.J. Sanderson, *Proceedings of ASM International Conference on Production, Fabrication, Properties and Application of Ferritic Steels for High Temperature Applications,* Warren, PA, October 6-8, 1981, ed. A.K. Khare, ASM, Metals Park, Ohio, (1983) 85.
4. G. Ebi and A.J. McEvily, *Fatigue Fract Engng Mater Struct* 17 (1984) 299.
5. V.K. Sikka, C.T. Ward and K.C. Thomas, *Ferritic Steels for High Temperature Applications*, *Proceedings of ASM International Conference on Production, Fabrication, Properties and Application of Ferritic Steels for High Temperature Applications,* Warren, PA, October 6-8, 1981, ed. A.K. Khare, ASM, Metals Park, Ohio, (1983) 65.
6. B.G. Gieseke, C.R. Brinkman and P.J. Maziasz, *Microstructure and Mechanical properties of Ageing Material,* eds. P.K. Liaw, R. Viswanathan, K.L. Murty, E.P. Simonen and D. Frear, The Minerals, Metals and Materials Society (1993) 197.
7. R.W. Swindman, *Low Cycle Fatigue*, *ASTM STP 942*, S.D. Solomon, G.R. Halford, L.R. Kaisand and B.N. Leis, Eds. (1998) ASTM, Philadelphia, 107.
8. Y. Asada, K. Dozaki, M. Ueta, M. Ichimiya, K. Mori, K. Taguchi, M. Kitagawa, T. Nishida, T. Sakon and M. Sukekawa, *Nucl Engng Des*.139 (1993) 269.
9. W.B. Jones, *Ferritic Steels for High Temperature Applications, Proceedings of ASM International Conference on Production, Fabrication, Properties and Application of Ferritic Steels for High Temperature Applications,* Warren, PA, October 6-8, 1981, ed. A.K. Khare, ASM, Metals Park, Ohio, (1983) 221.
10. A. Nagesha, M. Valsan, R. Kannan, K. Bhanu Sankara Rao, S.L. Mannan, *Int. J. Fatigue*, 24 12 (2002) 1285.

11. D. Eifler and D. Rottger, *Proc. 7th Int. Fatigue Congress, Fatigue '99*, June 1999, Beijing, Xue-Ren Wu and Zhong-Guang Wang, Eds. 4 (1999) 2145.
12. S. Nishino, K. Shiozawa, K. Takahashi, S. Seo and Y. Yamamoto, *Proc. 7th Int. Fatigue Congress, Fatigue '99*, June 1999, Beijing, Xue-Ren Wu and Zhong-Guang Wang, Eds. 4 (1999) 2177.
13. Data sheets on elevated temperature time-dependent low cycle fatigue properties of ASTM A387 Grade 91 (9Cr-1Mo) steel plate for pressure vessels, *NRIM* (data sheet No. 78).
14. S. Kim and J.R. Weertman, *Metall Trans* A 19 (1988) 999.
15. H. Okamura, R. Ohtani, K. Saito, K. Kimura, R. Ishii, K. Fujiyama, S. Hongo, T. Iseki and H. Uchida, *Nucl Engng Design* 193 (1999) 243.
16. T. Sugiura, A. Ishikawa, T. Nakamura and Y. Asada, *Nucl Engng Des*. 153 (1994) 87.
17. K. Aoto, R. Komine, F. Ueno, H. Kawasaki, and Y. Wada, *Nucl Engng Des*.153 (1994) 97.
18. L. Zhu, Q. Zhao, H. Gu and Y. Lu, *J. Mater. Sci. Tech* 14 (1998) 226.
19. M.Valsan, D.H.Sastry, K.Bhanu Sankara Rao and S.L.Mannan, *Metall. Trans*., Vol. 25A, 1995, p159.
20. K.Bhanu Sankara Rao, M.G.Castelli and J.R.Ellis, *Scripta Metall. Mater*., Vol.33, 1995, p1005.
21. M.G.Castelli, R.V.Miner, D.N.Robinson, ASTM STP 1186, ASTM, Philadelphia, 1993, p106.
22. S.Herenu, I.Alvarez-Armas, A.F.Armas, *Scripta Mater*., 45, 2001, 739-745.
23. K.Bhanu Sankara Rao, "Influence of Metallurgical Variables on the Low Cycle Fatigue Behaviour of Type 304 Stainless Steel", *Ph.D. thesis*, University of Madras, India, January 1989.
24. K.Tsuzaki, T.Hori, T.Maki and I.tamura, *Mater. Sci. Engng*, Vol.61 1983, p247.
25. A. Nagesha, M. Valsan, R. Kannan, K. Bhanu Sankara Rao, S.L. Mannan, *Proc. 9th Int. Conf. Mechanical Behavior of Materials*, Geneva, May 2003.
26. D.S. Wood, A.B. Baldwin and K. Williamson, *Proc. IAEA Meet on Time and Load Dependent Degradation of Pressure Boundary Materials*, Innsbruck, Nov. 1978, in Rep. of IWG RRPC 79/2 (1979) 88.
27. S.J. Sanderson and S. Jacques, *Proc. IAEA Specialist Meet on Mechanical Properties of Structural Materials Including Environmental Effects, Chester, October 1983* Vol. 2 in *Rep. IWGFR-49* IAEA (1984) 601.
28. W.B. Jones and J.A. Van Den Avyle, *Metall Trans* 11A (1980) 1275.
29. A. F. Armas, M. Avalos, I. Alvarez-Armas, C. Petersen, R. Schmitt, *J. Nucl. Materials 258-263 (1998) 1204-1208.*
30. K.D. Challenger and A.K. Miller, *J. Eng. Mater. Technol* ASME 103 (1981) 7.
31. T. Ogata and A. Nitta, *Proc. 30th Symposium on Structural Materials at High Temperature* (1992)149.

FIGURES

Fig. 1 Initial microstructure of N+T Modified 9 Cr- 1 Mo ferritic steel

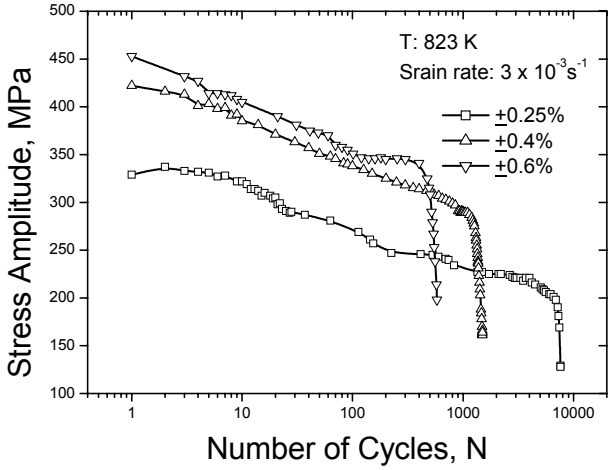

Fig. 2 Influence of strain amplitude on cyclic stress response at 823 K

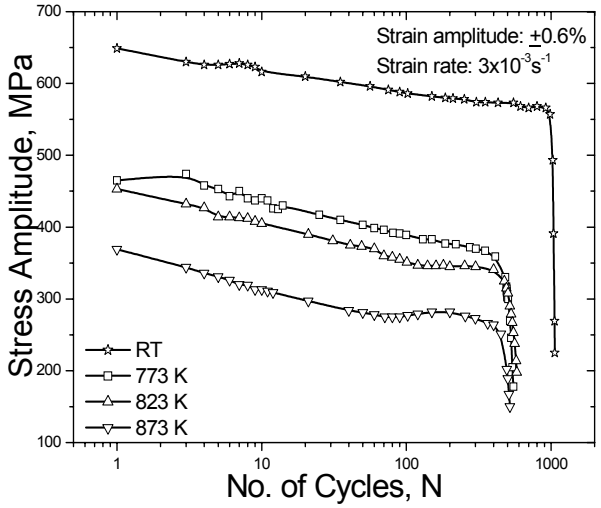

Fig. 3 Influence of temperature on cyclic stress response (±0.6%; 3×10^{-3} s^{-1})

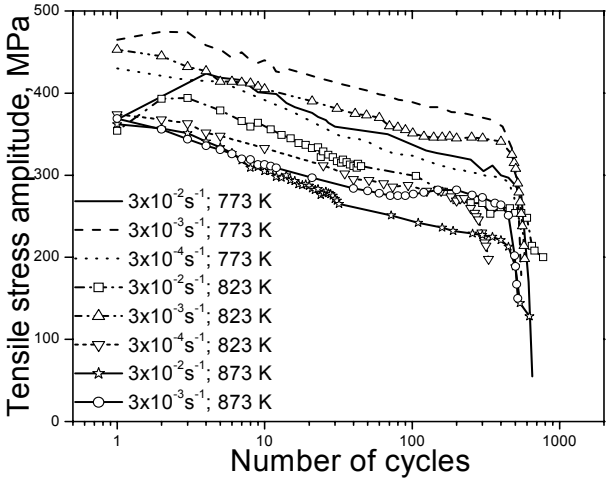

Fig. 4 Cyclic stress response - dependence on strain rate

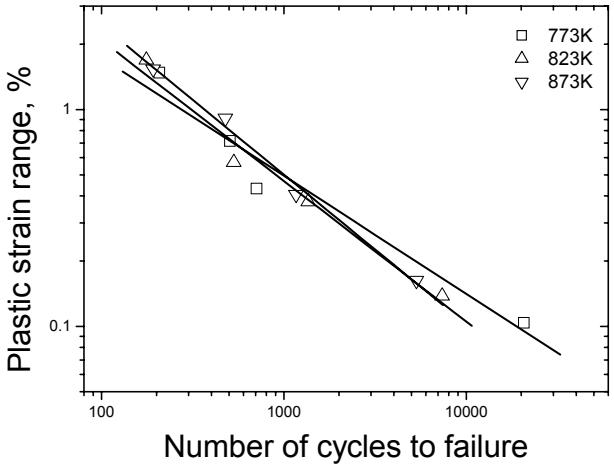

Fig. 5: Variation of LCF life with temperature

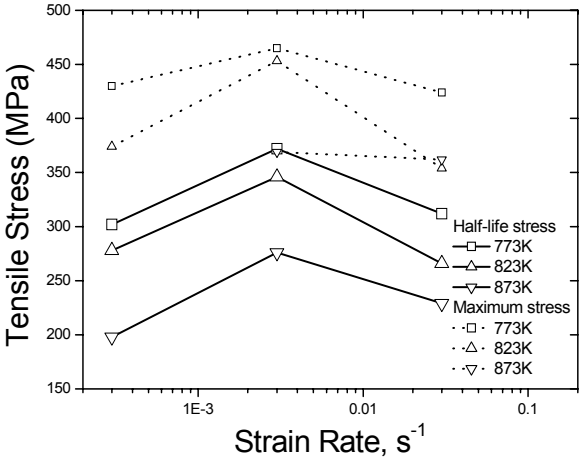

Fig. 6 Strain rate effect on maximum tensile stress and half-life stress

Table I: Half-Life plastic strain amplitudes and Peak tensile stress at half-life at different temperatures and strain amplitude and at constant strain rate of 3 x 10^{-3} s^{-1}

Total Strain Amplitude, $\Delta\varepsilon_t/2$ (%)	Plastic Strain Amplitude $\Delta\varepsilon_p/2$ (%)			Peak tensile stress at half-life (MPa)		
	773 K	823 K	873 K	773 K	823 K	873 K
0.25	0.05	0.07	0.08	238	221	180
0.40	0.21	0.19	0.20	346	303	274
0.60	0.36	0.28	0.46	372	346	276
1.00	0.74	0.85	0.77	357	293	259

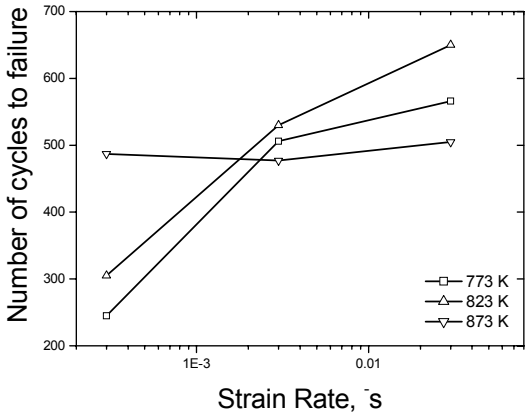

Fig. 7: Variation of LCF life with strain rate at different temperatures

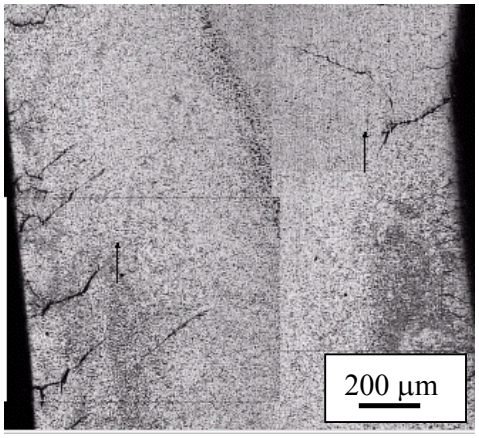

Fig. 8 (a) Crack propagation at 773 K at ±0.6% and 3×10^{-4} s^{-1} (arrows indicate the loading direction)

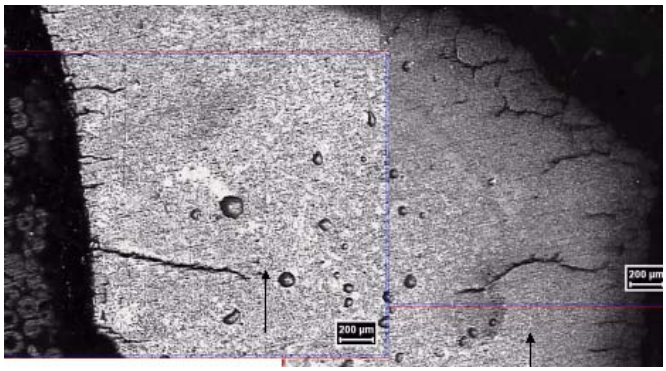

Fig. 8 (b) Crack propagation at 823 K at ±0.6% and 3×10^{-4} s^{-1}

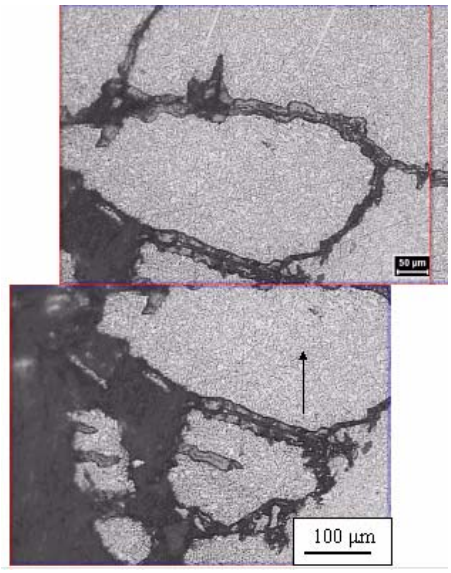

Fig. 8 (c) Test at 873 K, ±0.6% and 3×10^{-4} s^{-1}. Oxidation-assisted crack initiation and propagation.

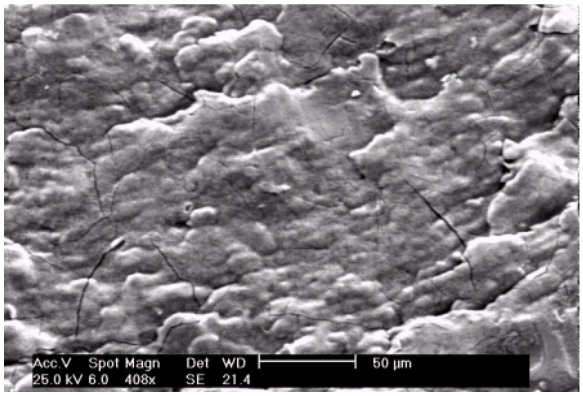

Fig. 9 Factograph showing oxidation assisted cracking during testing at 3×10^{-4} s^{-1} and 873 K